

Analysis, Control and Simulation of Switched Boost Network Inverter using Modified PWM approach for E-bike Applications

SARODE SHIVA KUMAR¹, GAURI SHANKER GUPTA², SUDHANSU KUMAR MISHRA³,
PANKAJ MISHRA⁴

^{1,2,3,4} Department of Electrical and Electronics Engineering, Birla Institute of Technology, Mesra,
Ranchi, 835215, INDIA.

Corresponding Author-shivkumar.ee@gmail.com

Abstract: - A transformer less with modified PWM approach control switched boost network inverter to supply the motor in the E-bike application is demonstrated in this work. The output received from battery is of low magnitude DC voltage, making it unsuitable for high power AC applications. Traditionally, to make the low power DC obtained suitable for high power AC applications, integration of boost chopper and conventional VSI is used, resulting in two stage conversion, making the overall system bulkier and more expensive, and unsuitable for low power consumptions. To address this issue, Z-source inverter (ZSI) can be used, but ZSI uses two LC pairs in its front stage, making the system bulkier. This paper presents a switched boost network inverter (SBNI) topology with features alike ZSI albeit without the detriment of a high component count and involves controlled shoot through operation without harming converters functionality. The steady state and small signal analysis of the proposed topology, as well as the proposed PWM strategy, are discussed. In the MATLAB/SIMULINK environment, the topology and proposed PWM technique are validated. The obtained results show a good significant relation between the theoretical and simulated waveforms.

Key-Words: - VSI (voltage source inverter), ZSI (Z-source inverter), SBNI (switched boost network inverter), steady state analysis, PWM strategy

Received: March 16, 2024. Revised: August 27, 2024. Accepted: September 17, 2024. Published: October 17, 2024.

1 Introduction

Due to the major concern on environment, climate variations and CO₂ emissions the major countries of the world are stepping forward towards the electrification of automobile industry. Subsequently, the electric vehicles are on the rising demand. The battery-operated vehicles are on majority of the stake as compared to total electric vehicles (EV's) production. Among different types of EV's, the two wheelers and three wheelers fall under the category of light EV's, and they play major role in the less maintenance cost as compared to other EV's like four wheelers. R. Caceres et al., published the first report on this single stage single-phase inverter in 1995 in [1]. This inverter employed single-stage voltage amplification and voltage inversion, with a total of four switches in [1]-[5] etc.,. However, the available solutions of control of boost converter with voltage source inverter does not comply with single stage conversion of supply to electric vehicle motor. Moreover, the available power converters interface with EV motor entertains two stages which lead to conversion losses and reduce the performance of the EV.

The conventional voltage source inverter has a wide range of applications in our daily lives, from uninterruptible power supply (UPS) systems to

injecting power into the grid, and is thought to serve all DC-to-AC conversion purposes. However, conventional VSI has the limitation of functioning in buck mode, which creates difficulties in meeting the high-power demand of diverse products. To make it suitable for high power applications, a boost chopper is integrated with the VSI, and the very first stage conversion involves DC-to-DC conversion, in which the low voltage DC voltage obtained from the battery bank is translated to a high DC voltage level to meet the users' needs, and the output terminal of the boost chopper is connected to the input side of the VSI. The VSI implements the DC-to-AC conversion operation, determining the final topology suitable for high power demand. Since the boost chopper coupled VSI had two stage conversion, it had low boost gain and more loss, so single stage conversion topologies were presented with a control scheme to overcome the two stage conversion drawbacks. These topologies accomplish voltage amplification and voltage inversion in a single stage. The basic operation of a single-stage single-phase inverter is to control two boost converters in such a way that the output voltage across the capacitor is of the AC type with the same level of DC offsets.

Recently, the design of boost inverters for EV applications, has become popular, and because these

use battery energy source as their primary source of electrical energy, they have attracted many scientific communities. The output of these devices is primarily a DC voltage, which must be converted into AC to be usable, which necessitates the use of an inverter which is being discussed in [6]-[9]. A modern study and analysis of a boost inverter, as discussed in [10]-[16], gives us an idea of the various types that exist in the design of a boost inverter. Other considerations when designing a boost inverter include electromagnetic interference (EMI), total harmonic distortion, noise, cost effectiveness, size, and many others. Common mode leakage current (CMLC) is an important factor to consider when designing a boost inverter for a EV-based application [17].

2 Problem Formulation

To overcome the conventional boost inverter's major drawbacks of high inrush current, high voltage stress, high component count, high switching losses, and low boost factor, another switched boost network inverter topology was presented in [18]-[21], where a novel shoot through approach was used to increase the boost factor of the proposed topology. Several other topologies were proposed in order to increase the boost factor of the boost inverter. Some of the proposed topologies for increasing the boost factor are presented in [19]- [23]. Undoubtedly, they increased the boost factor to a great extent, but at the cost of increased topology size and cost, which can be proven ineffective for lower power utility.

In order to increase the boost factor of a boost inverter, various topologies and control techniques have been proposed up to this point. This paper presents a topology of switched boost inverter that makes use of shoot through voltage, thereby controlling the topology in a novel way. Additionally, the presented topology has been controlled using a new close loop controller to reduce the possibility of error.

With the objective to minimize the above-mentioned limitations, a closed loop modified PWM approach incorporated in the switch boost network inverter is presented in this article. The main contributions of this work are as follows:

1. Transformer less modified PWM approach switch boost network inverter for EV application is analyzed and simulated for

the efficient, cost effective supplying the EV motor.

2. Simplified switch boost network inverter with single stage conversion topology is investigated by steady state analysis.
3. A modified PWM approach leading to stability is proposed in this article.
4. Overall converter is tested through simulation and performance is examined.

2.1 Block Diagram of Proposed system

The basic idea of how the proposed topology works is that initially battery power is harnessed, and the DC voltage is applied to switched boost network that aids in boosting the voltage. This network assists in increasing the low DC voltage to an appropriate level; the augmented DC voltage is then fed into the conventional VSI, which converts it to AC voltage and feed the motor.

In the open loop, control signals for all switches are generated using a sine wave as a reference signal, whereas in the closed loop, VSI output voltage (AC) is used as a reference signal via the feedback loop in addition to a sine wave, The error is compensated using a PI controller, and the resulting PI-controlled signal is used as the reference signal for the switches in the system, resulting in a more stable system. Fig 1 below represents the block diagram of the proposed system:

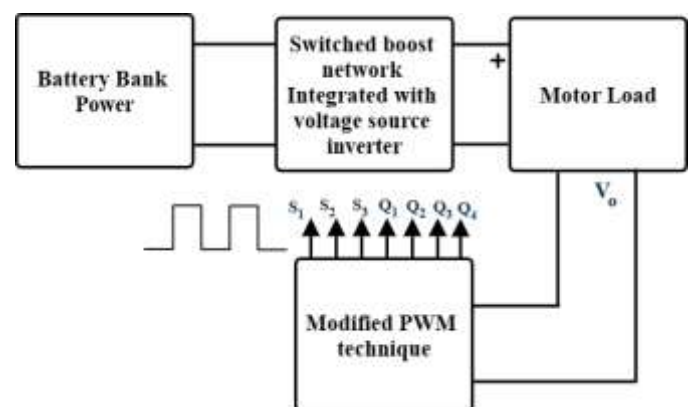


Fig. 1: Block diagram of proposed topology

3 Problem Solution

The presented topology incorporates all the advantages of the ZSI and attempts to overcome the disadvantages of the same as well as the topologies proposed thus far. Fig 2 depicts the circuit diagram of the presented topology.

The configuration of the converter consists of diodes D_a , switches S_1, S_2, S_3 , Inductor L and capacitor C , inverter switches Q_1, Q_2, Q_3, Q_4 .

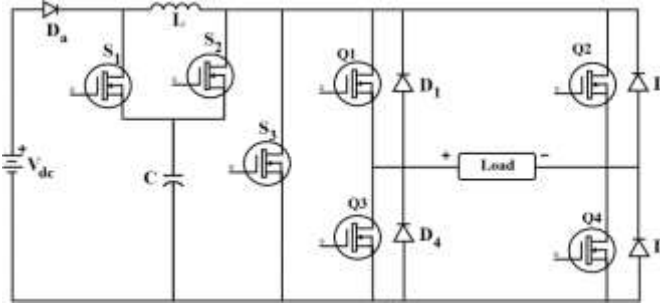


Fig 2: Circuit diagram of the topology

• Modes of operation

The presented topology has two modes of operation, which are outlined in this section:

Mode 1:

D_a : Reversed biased; S_1 : ON; S_2 & S_3 : OFF

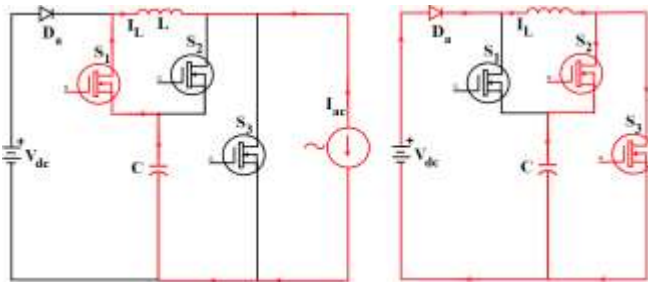


Fig 3 Modes of operation

In this mode of operation, switch ' S_1 ' is turned ON and switch ' S_2 and S_3 ' is turned off, indicating that the inverter is in a non-shoot through state. So the inverter is viewed as a current source, the duty cycle of this mode is written as DT_S or $(1-D_{S3})T_S$. In order to, elucidate the SBNI's steady-state operation, the inverter is assumed to be in a non-shoot-through zero state for duration $D.T_S$ in a switching cycle T_S , and is represented by a current-source. The diode D_a is reverse biased (as $V_C > V_{dc}$), and the capacitor C charges the inductor L through the inverter bridge and switch S_1 . In this interval, the inductor current equals the capacitor discharging current.

Mode 2:

D_a : forward biased; S_1 : off; S_2 and S_3 : on

This mode of operation begins when switch ' S_1 ' is turned off and switches ' S_2 and S_3 ' are turned on, indicating that the inverter is in shoot-through mode and the inverter leg is short-circuited, so the duty cycle of this mode is given as $(1-D)T_S$ or $D_{S3}T_S$. For the remaining period of the switching cycle $(1-D).T_S$, the inverter is in shoot-through mode and the inverter bridge is represented by a short-circuit. Now, the voltage source V_{dc} and inductor L work together to power the inverter and capacitor through diode D_a . In this interval, the inductor current equals the capacitor charging current. It should be noted that the inductor current is assumed to be sufficient for the continuous operation of diode D_a over the entire interval $(1-D).T_S$.

Figure 4 depicts key steady-state converter waveforms that vary with respect to the gate pulse S_1 of switch S_1 and S_2 and S_3 of switch S_2 and S_3 .

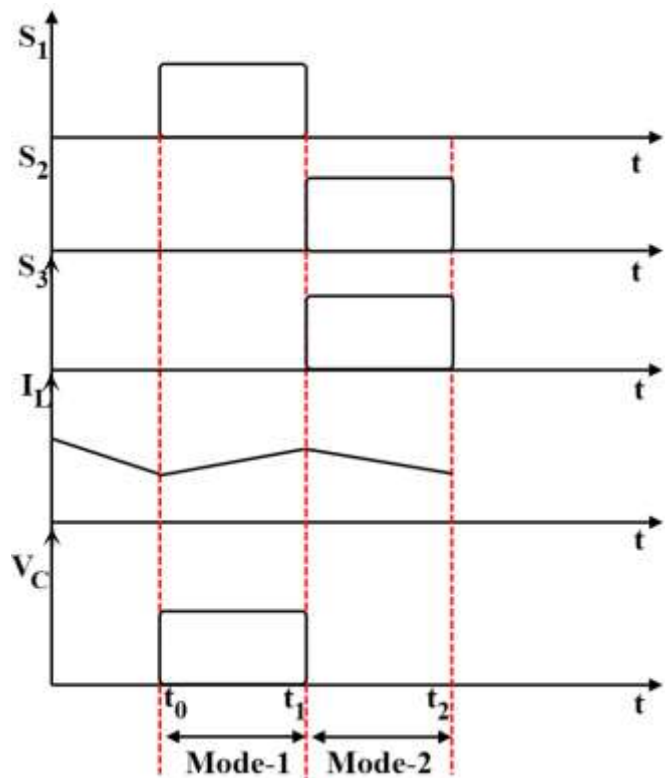


Fig 4 Key Steady state waveforms of the topology

The following is the relevant mathematical analysis of the modes of operation of the topology

$$V_L = V_C; 0 < t < DT_S$$

$$V_L = V_G - V_C; DT_S < t < T_S \quad (1)$$

$$i_C = \begin{cases} -i_L - i_I; 0 < t < DT_S \\ i_L - i_I; DT_S < t < T_S \end{cases} \quad (2)$$

$$V_i = V_C; 0 < t < DT_S$$

$$\begin{cases} 0; DT_S < t < T_S \end{cases} \quad (3)$$

OR

$$V_L = \begin{cases} V_G - V_C; 0 < t < D_{ST}T_S \\ V_C; D_{ST}T_S < t < T_S \end{cases} \quad (4)$$

$$i_C = i_L - i_I; 0 < t < D_{ST}T_S$$

$$\begin{cases} -i_L - i_I; D_{ST}T_S < t < T_S \\ 0; 0 < t < D_{ST}T_S \\ V_C; D_{ST}T_S < t < T_S \end{cases} \quad (5)$$

$$\quad (6)$$

In one switching cycle, the average voltage across the inductor and the average current across the capacitor should be equal to zero. So, using the volt-second balance law for average inductor voltage, considering switch S_1 , we get:

$$V_C D + (V_{dc} - V_C)(1 - D) = 0$$

$$\frac{V_C - 1 - D}{V_{dc} - 1 - 2D} \quad (7)$$

For switch S_3 :

$$(V_{dc} - V_C)D_{S3} + V_C(1 - D_{S3}) = 0$$

$$\frac{V_C - D_{S3}}{V_{dc} - 1 + 2D_{S3}} \quad (8)$$

Similarly, applying the charge-second balance law to capacitor current yields:

Considering switch S_1

$$(-i_L - i_I)D + (i_L - i_I)(1 - D) = 0$$

$$\frac{i_L - 1}{i_I - 1 - 2D} \quad (9)$$

Considering switch S_3

$$(-i_L - i_I)(1 - D_{S3}) + (i_L - i_I)D_{S3} = 0$$

$$\frac{i_L - 1}{i_I - 2D_{S3} - 1} \quad (10)$$

The conversion ratio (V_C/V_{dc}) expression for switch S_1 and switch S_3 , for switch S_1 is unity when $D = 0$ and becomes very high as D approaches 0.5, whereas (V_C/V_{dc}) for switch S_3 is 0 when $D_{S3} = 0$ and increases with increase in D_{S3} as D_{S3} approaches 0.5. It should be noted that, analogous to a ZSI, the SBI's non-shoot through duty ratio (D) and shoot-through duty ratio (D_{ST}) cannot exceed 0.5.

3.1 Small-Signal Analysis

The state-space averaged model of the proposed topology is given by :

$$K.\hat{x} = A\hat{x} + B\hat{u} \text{ and } \hat{y} = C\hat{x} + D\hat{u} \quad (11)$$

Where,

$$\hat{x} = \begin{bmatrix} \hat{i}_L \\ \hat{V}_C \end{bmatrix} ; \hat{u} = [\hat{V}_{dc}] ; \hat{y} = [\hat{V}_o]$$

$$A = \begin{bmatrix} 0 & \frac{2D-1}{L} \\ \frac{1-2D}{C} & -\frac{D}{C} \end{bmatrix} ; B = \begin{bmatrix} 1-D \\ L \\ 0 \end{bmatrix} ; C = [0 \quad D]$$

$$D = [0]$$

So, now the open-loop transfer function is:

$$C[SI-A]^{-1}B = \frac{\frac{2D^2 - 3D + 1}{LC}}{S^2 + S\frac{D}{C} - \frac{1-4D^2}{LC}} \quad (12)$$

Similarly close loop transfer function (C.L.T.F) for the simplified block diagram of the presented topology is obtained as:

$$\text{C.L.T.F} = \frac{G(s)}{1 + G(s)H(s)}$$

$$G(s) = \frac{\frac{2D^2 - 3D + 1}{LC}}{S^2 + S\frac{D}{C} - \frac{1-4D^2}{LC}}$$

$$H(s) = \frac{1}{24}$$

$$C.L.T.F = \frac{\frac{2D^2 - 3D + 1}{LC}}{s^2 + s\frac{D}{C} - \frac{1-4D^2}{LC}} \cdot \frac{1}{1 + \frac{2D^2 - 3D + 1}{LC} \cdot \frac{1}{s^2 + s\frac{D}{C} - \frac{1-4D^2}{LC}}} \quad (13)$$

3.1.1 PWM Generation

Fig 5 portrays the PWM generation for the gating pulses of SBNI's switches (S₁ and S₂ & S₃) and inverter switches Q₁, Q₂, Q₃ and Q₄.

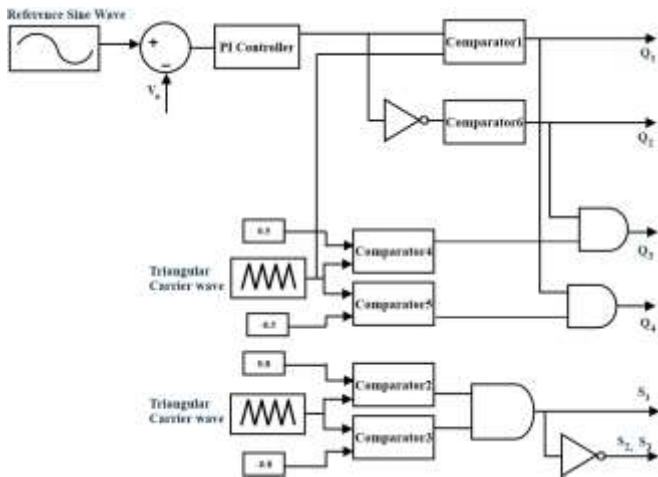


Fig 5: Modified PWM technique

To commence the generation of the modulated signal, a reference sine wave, positive and negative duty cycle ($D=20\%$) signals of switch S₁, and positive and negative duty cycle ($D_{S3}=50\%$) signals of switch S₂ and S₃ are obtained, the output of which is the modulated signal, as shown in fig 6. Similarly, for the generation of gating pulses for switches 'S₁', 'S₂ and S₃', The positive and negative duty cycles are compared with the carrier triangular signal and the output of the comparator generates the PWM gating pulse signal for the switch 'S₁', as shown in fig 6, and because the switches 'S₁' and 'S₂ and S₃' work with a 180° phase difference, gating pulses for the switch 'S₂ and S₃' generated and are complimentary with respect to S₁.

Fig 7 juxtaposes and are the simulated waveforms obtained for all three switches of switched boost network in the MATLAB/SIMULINK environment.

3.1.2 Results

The presented topology with the modified PWM technique, is simulated in the MATLAB/SIMULINK environment and is used to validate the proposed PWM technique. Table-1 lists the parameters used in the simulation. For current topology close loop control, a conventional PI controller is used. Fig 7 shows the simulation waveform of gate pulses of switches 'S₁' and 'S₂ and S₃' and validates the theme of fig 5. Fig 8 depicts the inverter switch 'Q₁', 'Q₂', 'Q₃' and 'Q₄' gate pulses out of the proposed modulation technique. Fig 9 represents the inductor current simulated waveform within the range of current limit in the switched boost network topology. Fig 10 shows the capacitor voltage of the switched boost network topology, the ripple voltage is within the permissible limits. From Fig 9 and 10, it is evident that the waveforms are in accordance with the theory cited in section II modes of operation. Fig 11 portrays the load voltage and current which is evident that the proposed system converts DC to AC and simultaneously boosts the voltage.

The uptick in supply voltage demonstrates that the proposed topology is effective in enhancing voltage to the appropriate level.

From fig 11 the final output obtained by using the presented topology and modified PWM technique, it can be seen that the output voltage obtained(45V) is 87.5% more than that of the input voltage thus the result obtained verifies the theory cited above. Fig 12 shows the simulation result of the total harmonic distortion (THD) of load which is within the permissible limits as per the IEEE standards. From the simulation results it is evident that the network can be of value in terms of a E bike motor application.

Table-1 Parameters used for the validation of simulation of the proposed system.

V_{DC}	24V
D(S), D_{ST}(S_t)	20%, 50%
Sine wave frequency	50 Hz

Carrier signal frequency	10kHz
SBN inductor	1mH
SBN capacitor	20 μ F
LC filter	30mH, 650 μ F
Feedback loop	1/24
PI controller values	P= 0.585, I=702
V_{OUT}	45V

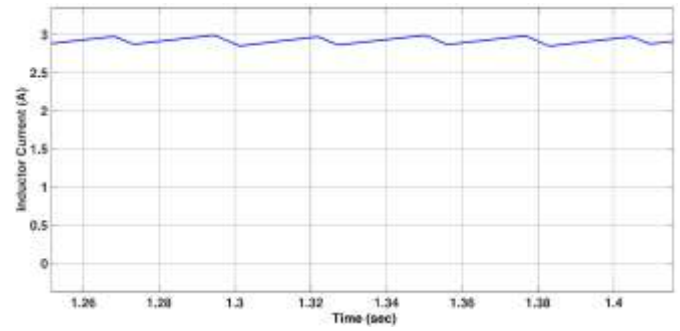


Fig 9: Simulation result of Inductor current of Switched Boost Network

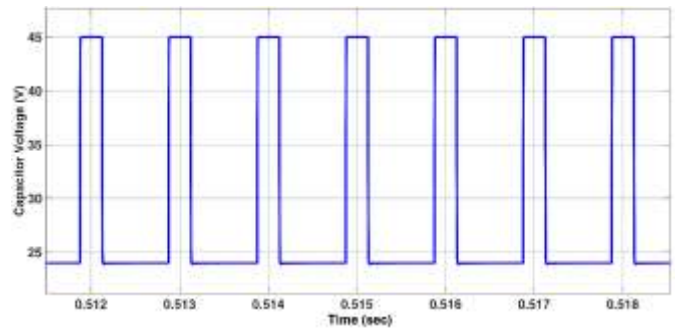


Fig 10: Simulation result of Capacitor voltage of Switched Boost Network

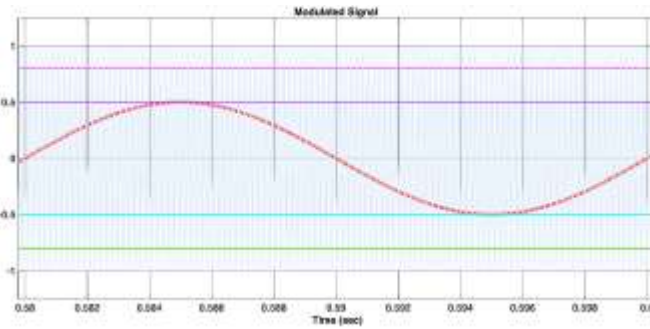


Fig. 6 Modulated wave

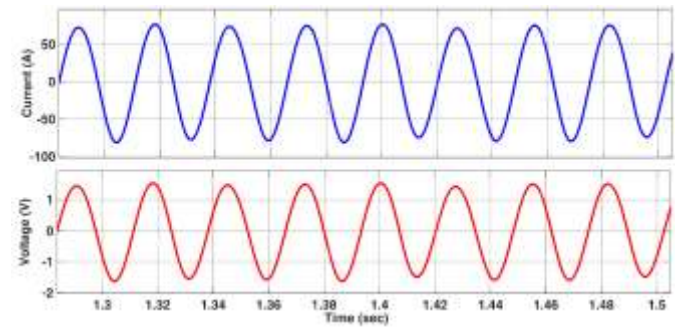


Fig 11: Simulation result of Output Voltage and Current of the presented system

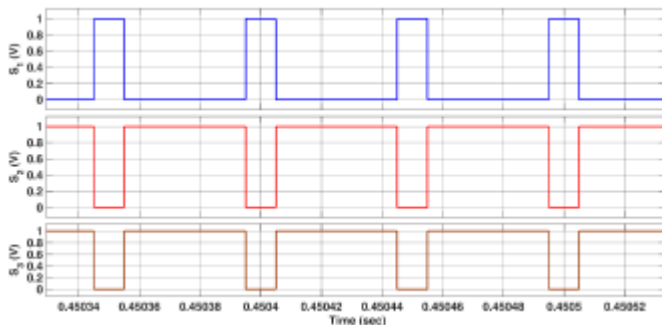


Fig 7: Gate pulses for switch 'S₁' and switch 'S₂ and S₃'

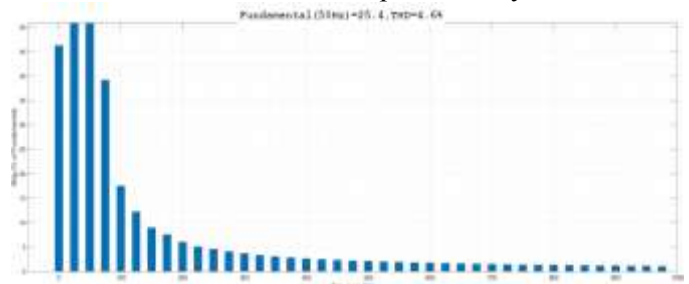


Fig 12: Simulation result of Total harmonic distortion(THD) of the proposed system

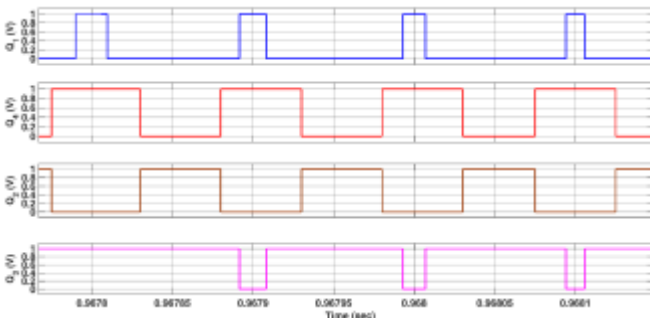


Fig 8: Gate pulses for inverter switches

4 Conclusion

In this article a modified PWM technique is employed in the switch boost network-based inverter to eliminate the two-stage conversion issue. The proposed system directly converts DC to AC and boost the voltage to the required level of E-bike motor application. In this as the conversion process is achieved in single stage as compared to conventional process with reduced number of components as it is apparent from the topological configuration, which makes it a cost-effective solution. The current work is basically focused on mechatronics of E-bike application. It is proved from the results that the process of conversion is minimized along with boosting the voltage levels. From the results and operation, it is clear that the controlled shoot through claim is achieved. Furthermore, the proposed system is simple low cost and has ease of control features.

References:

- [1] R. Caceres and I. Barbi, "A Boost DC-AC converter: operation, analysis, control and experimentation," in *Industrial Electronics, Control, and Instrumentation, 1995., Proceedings of the 1995 IEEE IECON 21st International Conference on*, vol. 1.1995, pp. 546–551.
- [2] H. S. Das, C. W. Tan, A. H. M. Yatim, and N. D. bin Muhamad, "Analysis and control of boost inverter for fuel cell applications," in *Power and Energy (PECon), 2016 IEEE International Conference*, 2016, pp. 455–460.
- [3] T. Sreekanth, N. Lakshminarasamma, and M. K. Mishra, "Coupled inductor-based single-stage high gain DCAC buck-boost inverter," *IET Power Electronics*, vol. 9, no. 8, pp. 1590–1599, 2016.
- [4] A. Kumar and P. Sensarma, "A Four-Switch Single-Stage Single-Phase Buck Boost Inverter," *IEEE Transactions on Power Electronics*, vol. 32, no. 7, pp. 5282–5292, Jul. 2017.
- [5] A. Ravindranath, S. K. Mishra and A. Joshi, "Analysis and PWM Control of Switched Boost Inverter," in *IEEE Transactions on Industrial Electronics*, vol. 60, no. 12, pp. 5593-5602, Dec. 2013.
- [6] Mohsen Hasan Babayi Nozadian, Ebrahim Babaei and Vida Ranjbarzad "Steady State Analysis of Dual Switched Boost Inverter," *2018 IEEE 12th International Conference on Compatibility, Power Electronics and Power Engineering (CPE-POWERENG 2018)*.
- [7] Tomoya Sugimoto, Takahiro Nozaki and Toshiyuki Murakami "Extended T-Type Boost Inverter Using Switched Capacitors," *IECON 2019 - 45th Annual Conference of the IEEE Industrial Electronics Society*.
- [8] E. Babaei, E. Shokati Asl, M. Hasan Babayi, and S. Laali, "Developed embedded switched-Z-source inverter," *IET Power Electron.*, vol. 9, no. 9, pp. 1828–1841, July 2016.
- [9] M.K. Nguyen, T.V. Le, S. J. Park, and Y. C. Lim, "A class of quasi switched boost inverters," *IEEE Trans. Ind. Electron.*, vol. 62, no. 3, pp. 1526–1536, March 2015.
- [10] E. S. Asl, E. Babaei, M. Sabahi, et al, "New half-bridge and full-bridge topologies for switched-boost inverter with continuous input current," in *IEEE Transactions on Industrial Electronics*, vol. 65, no. 4, pp. 3188- 3197, 2018.
- [11] F. A. A. Meinagh, E. Babaei, and H. Tarzarni, "Modified high voltage gain switched boost inverter," in *IET Journals & Magazines*, vol. 10, no. 13, pp.1655-1664, 2017.
- [12] R. Priya, R. Valli and P.L. Santhana Krishnan "Single Stage Dual Boost Inverter with Half Cycle Modulation Scheme for PV System Applications," *2019 IEEE International Conference on System, Computation, Automation and Networking (ICSCAN)*.
- [13] Anil Gambhir and Santanu Mishra, "Gain Enhancement of Switched Boost Inverter using a Novel PWM Scheme," *2019 IEEE Energy Conversion Congress and Exposition (ECCE)*
- [14] Masoud Ghodsi and Seyed Masoud Barakati, "A New Switched Boost Inverter Using Transformer Suitable For The Microgrid-

- Connected PV With High Boost Ability,” 2016 7th Power Electronics and Drive Systems Technologies Conference (PEDSTC).[15] Sreeram K., “Design and Development of Differential Boost inverter Fed Induction Motor Drive,” 2018 International Conference on Circuits and Systems in Digital Enterprise Technology (ICCSDET)
- [15] Zhixiang Yu, Xuefeng Hu, Zhilei Yao, Lezhu Chen, Meng Zhang and Shunde Jiang, “analysis and design of transformerless boost inverter for standalone photovoltaic generation system,” *CPSS Transactions on Power Electronics and Applications*, vol 4, no 4, December 2019.
- [16] L. Zhang, X. B. Ruan, and X. Y. Ren, “The control method of the front stage DC converter in the two stage inverter,” in *Proceedings of the CSEE*, vol. 35, no. 3, pp. 660-670, 2015
- [17] K. Jha, S. Mishra, and A. Joshi, “High-quality sine wave generation using a differential boost inverter at higher operating frequency,” in *IEEE Transactions on Industry Applications*, vol. 51, no. 1, pp.373-384, 2015
- [18] L. Qin, M. Hu, D. C Lu, Z. Feng, and Y. Wang, “Buck-boost dual-leg integrated step-up inverter with low THD and single variable control for single-phase high-frequency AC microgrids,” in *IEEE Transactions on Power Electronics*, vol. 33, no. 7, pp. 6278-6291, 2018.
- [19] A. Alexander and S. Keyue, “High-gain single-stage boosting inverter for photovoltaic applications,” in *IEEE Transactions on Power Electronics*, vol. 31, no. 5, pp. 3550-3558, 2016.
- [20] A. -T. Huynh, A. -V. Ho and T. -W. Chun, "Switched-Capacitor-Inductor Active-Switched Boost Inverters With High Boost Ability," in *IEEE Access*, vol. 9, pp. 101543-101554, 2021.
- [21] T. -D. Duong, M. -K. Nguyen, T. -T. Tran, Y. -C. Lim and J. -H. Choi, "A Switched-Boost Four-Leg Inverter With Leakage Current Mitigation," in *IEEE Transactions on Industrial Electronics*, vol. 71, no. 7, pp. 7210-7219, July 2024.
- [22] Rahim Samanbakhsh et al., “A Z-source inverter with switched network in the grid-connected applications,” *International Journal of Electrical Power & Energy Systems*, vol. 147, pp. 108819, May 2023.

Contribution of Individual Authors to the Creation of a Scientific Article (Ghostwriting Policy)

The authors equally contributed in the present research, at all stages from the formulation of the problem to the final findings and solution.

Sources of Funding for Research Presented in a Scientific Article or Scientific Article Itself

No funding was received for conducting this study.

Conflict of Interest

The authors have no conflicts of interest to declare that are relevant to the content of this article.

Creative Commons Attribution License 4.0 (Attribution 4.0 International, CC BY 4.0)

This article is published under the terms of the Creative Commons Attribution License 4.0

https://creativecommons.org/licenses/by/4.0/deed.en_US